Power Grid Frequency Monitoring over Mobile Platforms

Haoyang Lu, Lingwei Zhan, Yilu Liu and Wei Gao
Department of Electrical Engineering and Computer Science
University of Tennessee, Knoxville, Tennessee 37996-2250
Email:{hlu9,lzhan,liu,weigao}@utk.edu

***Abstract*—Information about the frequency deviation is critical to reliable and stable operation of the power grid. Current wide-area power grid monitoring systems consist of Phasor Measurement Units (PMUs) at both high-voltage transmission level and low-voltage distribution level, but are generally unsatisfactory for large-scale deployment over highly distributed microgrids in individual households and local communities due to their high cost and low accessibility. In this paper, we present a practical system design which significantly improves the accessibility and reduces the cost of frequency monitoring by unleashing the capabilities of modern mobile platforms in computation, communication, and storage. In our system, the Network Time Protocol (NTP) is exploited for time synchronization, replacing inflexible GPS receivers that are widely used in current PMUs. A small quantity of peripheral hardware components are used to build up an embedded sensing component for efficient and accurate frequency measurement. The experiment results compared to the traditional Frequency Disturbance Recorders (FDRs) show the effectiveness of the proposed frequency monitoring system.**

I. Introduction

Power grid is a critical infrastructure of the modern society, but is susceptible to various types of disturbances. When a significant disturbance occurs, the frequency of the power grid varies in both time and space, and, in many ways, exhibit the characteristics of electromechanical wave propagation phenomenon [1]. Therefore, information about the frequency deviation is particularly important to and highly desired for reliable and stable power grid operations.

How to obtain the frequency information more accurately and efficiently has been an active research topic for decades. Current power grid monitoring systems allow direct measurement of frequency and voltage phase angle by installing Phasor Measurement Units (PMUs) at either high-voltage transmission level [2] or low-voltage distribution level [3]. In particular, as a member of the PMU family, the Frequency Disturbance Recorders (FDRs), were developed in 2003 and deployed at the low-voltage distribution level such as 120V wall outlet with significantly reduced costs. Based on these FDRs, a US-wide Frequency Monitoring Network (FNET) has been designed, implemented, and deployed [4], enabling many applications of power system monitoring, control, and management. It is expected that 2,000 FDR units will be deployed worldwide in the next few years.

This work was supported in part by the Engineering Research Center Program of the National Science Foundation and the Department of Energy under NSF Award Number EEC-1041877 and the CURENT Industry Partnership Program. Pending provisional patent has been filed by the University of Tennessee.

These power grid monitoring systems, although having been proved to be effective in wide-area power grid infrastructure, are generally considered unsatisfactory for monitoring the operating status of the newly emerging distributed power systems, so-called microgrids [5]. Microgrids enable local integration of energy generation, distribution, and storage at the consumer level for better power system efficiency and control of demand [6]. The obstacles of efficient monitoring of microgrid operations mainly stem from the high installation cost and low accessibility of current PMUs, which prevent large-scale deployment of PMUs into individual households in high volume. For example, the installation cost of one PMU at the transmission level was more than $80,000 at the Tennessee Valley Authority (TVA). These PMUs are not intended for use at the distributed consumer level, and require professional installation which reduces end-users' incentives of having PMUs in their home energy systems.

In this paper, we present a practical system design which bridges the gap between current power grid monitoring systems and the unique requirements of microgrid monitoring, by fully unleashing the unexploited capabilities of modern mobile platforms, particularly smartphones, in computation, communication, and storage. The requirements of such monitoring on accurate time synchronization, high-resolution sensing, and real-time data processing, however, make it challenging to migrate the existing frequency estimation algorithm onto mobile platforms. First, power grid operations should be monitored in real-time using globally synchronized timestamps, so that measurements from dispersed locations can be compared on a common time reference [7]. Traditional PMUs rely on continuous analog signal reception from the GPS system for accurate timing, but have limited use for microgrids due to their large form factor, high cost, and inability for indoor scenarios. Second, with the increasing resolution and responsiveness of frequency monitoring, the workload of processing measurement data may exceed the computational capacity of current mobile systems, which are not intended for such real-time data processing. Specialized DSP chips are used in present PMUs for data processing [3], but are too expensive and difficult to be integrated into mobile platforms.

Our main idea to overcome the aforementioned challenges is to reduce the systematic cost of frequency monitoring by developing efficient embedded sensing platforms and adopting GPS-free time synchronization methods, without impairing the accuracy of AC waveform measurement and frequency

estimation. Our detailed contributions are as follows:

- We implemented a low-cost frequency monitoring prototype on the smartphone platform with a small quantity of peripheral hardware, which can be further integrated into the smartphone charger for better flexibility and convenience. The highly-integrated system lowers both the manufacturing and installation costs of the frequency monitoring system.
- We proposed a novel time synchronization approach based on the Network Time Protocol (NTP), which significantly increases the system flexibility by eliminating the requirement of GPS reception and line of sight to the satellites. The NTP timing information is used for both providing global timestamps and calibrating the local clock at smartphones.
- We developed a user-friendly graphic interface for frequency monitoring, as a smartphone application. The visualization of monitoring results would facilitate the understanding of end users. The extendibility of such interface also enables further integration of more power grid monitoring functionalities, such as phase angle and power quality monitoring, into the same platform.

The rest of this paper is organized as follows. Section II discusses the background knowledge of power grid frequency monitoring. Section III discusses the motivation for using mobile platform for PMUs. Section IV provides an overview of our system design. Section V presents our time synchronization approach based on NTP. Section VI presents our performance evaluation results in comparison with FDRs. The related work is depicted in section , respectively. Finally, the conclusions and future work are drawn in Section VIII.

II. Background

A. GPS-based Time Synchronization

Synchronization among different PMUs is important for wide-area power system frequency measurement. Each measurement must be assigned a timestamp for lateral comparison with measurements retrieved from other devices. To enable the global synchronization and timing accuracy, the Pulse-Per-Second (PPS) signal being retrieved from GPS receivers are usually used as the timing signal by PMUs [8][1]. The PPS signal is an analog output signal with a rising edge at each one second boundary of the Universal Coordinated Time (UTC). Since the precision of PPS signal is in nanoseconds with non-accumulative time drift [9], PMUs at dispersed locations can measure local system frequency synchronously using the integrated GPS clock. For example, a FDR would start a new 1-sec measurement cycle each time when it receives the PPS signal, and then transmits the frequency monitoring results back to FNET every 100ms for visualization. Such a monitoring result is calculated based on the AC waveform samples during the past 100ms, and is assigned to the timestamp of the first sample during this time period. For example, when the sampling frequency is 1,440 Hz and the current PPS rising edge corresponds to UTC time 17:05:04, the 144 samples generated between 17:05:04.1 and 17:05:04.2 are used to measure the system operating frequency, which is assigned to the timestamp 17:05:04.1. The FDR's local clock is used for sampling between two PPS rising edges.

[1]In the rest of the paper, the PPS signal and GPS signal are used interchangeably.

B. Time Synchronization via NTP

For better accessibility and lower cost, less expensive yet accurate and reliable timing sources have been studied in recent years. With nearly no cost, Network Time Protocol (NTP) [10] becomes an alternative timing source of GPS. Due to the uncertainty of network delay, the timing precision of NTP is in the order of 10ms [11], which is much lower than the PPS signal. However, by investigating the sample events recorded by FNET, we observe that this time precision is sufficient for detecting a frequency disturbance event. Being different from the PPS signal which continuously feeds the processor, the NTP timing information is only available when the monitoring device sends a request to the remote NTP server. The uncertain round-trip delay, therefore, further complicates the design of time synchronization method.

C. Frequency Estimation Algorithm

The operating frequency of the power grid could be computed from the rate of change of fundamental phase angles, and we have developed phasor-based methods for such computation [12]. The basic idea is to build on the theory of symmetrical components, and perform recursive Discrete Fourier Transform (DFT) calculations of the positive sequence voltage for a balanced system at a frequency different from the nominal frequency f_0 (e.g., 60 Hz) [13]. Given N data points of voltage waveform $\{x_k\}, k \in [1, N]$ per cycle of f_0, the phasor of the fundamental frequency component is

$$\begin{aligned}\overline{X}_1 &= \frac{1}{\sqrt{2}}\left(\frac{2}{N}\sum_{k=1}^{N} x_k \cos(\frac{2k\pi}{N}) - j\frac{2}{N}\sum_{k=1}^{N} x_k \sin(\frac{2k\pi}{N})\right) \\ &= \frac{1}{\sqrt{2}}(X_c^{(1)} + j \cdot X_s^{(1)}),\end{aligned}$$

and we can recursively compute each successive $(k+1)$-th phasor from the k-th phasor and data points x_{k+1} and x_{k+1-N}. The angle of the k-th phasor is given by $\phi(k) = \tan^{-1}(-X_s^{(k)}/X_c^{(k)})$, and we compute the operating frequency as $f_1 = f_0 + \Delta f = \frac{1}{2\pi} \cdot \frac{d\phi}{dk}$ through least-square approximation. Afterwards, to further improve the accuracy, f_1 is used to resample the voltage waveform and perform another correction $\Delta f'$, which is calculated from mathematical interpolation by maintaining a constant number of data points per sampling cycle. The final frequency is measured as $f_2 = f_1 + \Delta f'$.

III. Motivation

Modern mobile platforms, especially smartphones, are considered as an ideal platform for PMUs. As an example of low-cost PMUs, the FDR device includes a DSP chip to implement the real-time frequency estimation algorithm, a specialized ethernet module to upload the monitoring result to the server,

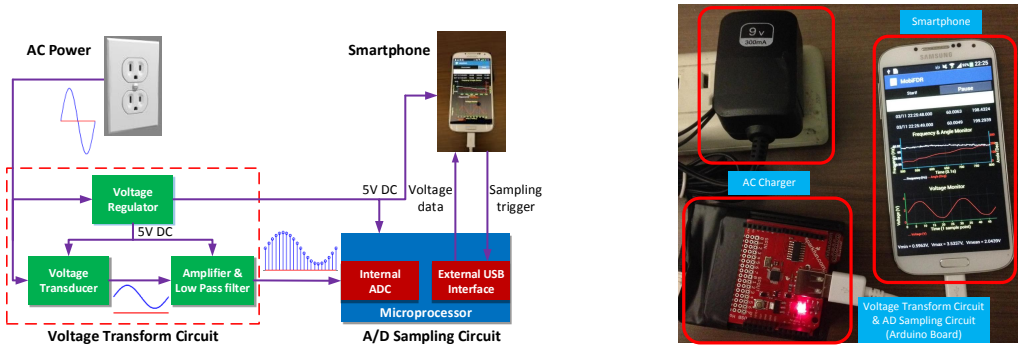

(a) System design (b) System implementation

Fig. 1. Power grid monitoring over mobile platforms

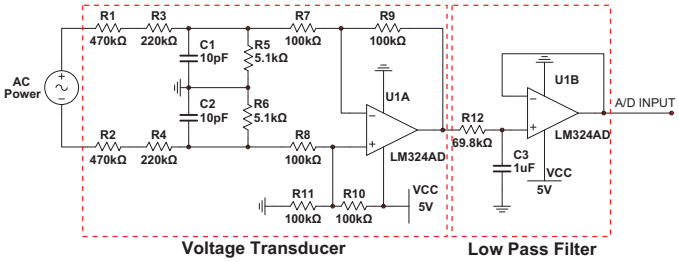

Fig. 2. Design of the voltage transform circuit

and a LCD module to display the monitoring results to end users. The aforementioned components have all been provided by modern smartphones. With the rapid development of IC and semiconductor manufacturing, the cost of a smartphone has been significantly reduced, and faster CPUs and more functionalities are integrated into the smartphone platform. For example, the Samsung Nexus S smartphone, with a price around 100 dollars, is equipped with 1 GHz ARM Cortex-A8 CPU, 512 MB RAM, 4.0-inch LCD screen, WiFi connection and cellular network access. These capabilities, together with its accessibility, make the modern smartphones an ideal choice for implementing the microgrid monitoring systems.

IV. System Design

A. Hardware design

Our developed frequency monitoring system consists of a voltage transform circuit, a microprocessor (MCU) module and an Android-based smartphone. The system design and implementation are shown in Fig. 1(a) and Fig. 1(b), respectively. The voltage regulator part outputs the 5V DC power to power up the smartphone, MCU module and the amplifiers. A voltage transform circuit, as shown in Fig. 2, takes an analog voltage signal from 120V wall outlet and transforms the AC power into the voltage range for analog-to-digital conversion (ADC) purpose. A low-pass filter with 230 Hz cut-off frequency rejects high-frequency noise. An 8-bit microprocessor ATmega328 (Arduino Uno board) with 10-bit internal ADC is then used to sample the voltage waveform at the sampling frequency of 1,440 Hz, and send the raw data to smartphone every 100 ms for processing.

The communication between the MCU and the smartphone is conducted by the USB host controller IC MAX3421E (USB host shield) [14]. The MAX3421E host controller contains the digital logic and analog circuitry necessary to implement a full-speed host compliant to USB specification v2.0. Under this circumstance, the smartphone behaves as USB slave in relation to the USB host chip, and can communicate with the MCU. The smartphone behaves as being connected to the desktop computer and will be charged while being connected to the USB host controller. The MCU communicates with the USB host shield through serial peripheral interface (SPI) bus.

B. Software design

At the smartphone, the frequency estimation algorithm and visualization programs are packaged into one Android application. To keep the application responsive, each computationally intensive operation such as the frequency computation specified in Section II-C, are distributed to a newly generated application thread, instead of residing in the application main thread or UI thread. As shown in Fig. 3, our frequency monitoring application consists of four major components, which are explained in detail as follows:

1) **USB communication component.** Through the USB connection, the smartphone will send the sampling trigger command every 2 seconds to the MCU, and the MCU will respond with the sampled measurement data. Our application will also monitor the connection status of the USB accessory. Once the smartphone is connected to the USB host controller with a correct hardware signature, our application will run automatically and build the USB connection as “plug-and-play”.
2) **Internet access component.** Network access is necessary to obtain the NTP timing information. The UTC timestamp is retrieved by requesting the NTP server. In addition, the measurement information is uploaded via the Internet to FNET servers hosted in the University of Tennessee. Since the network delay is uncertain and may be up to several hundred milliseconds, the network connection is packaged into one standalone thread.
3) **Frequency estimation component.** The frequency estimation algorithm described in Section II-C is implemented in this component. The MCU will store the sampled data within the last 0.1 seconds and send them to the smartphone at one time. Once these 144 samples

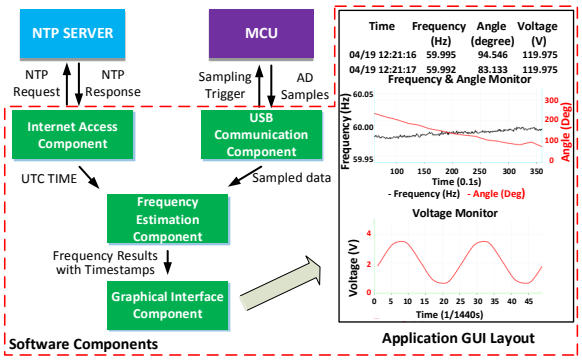

Fig. 3. Software components in the Android application

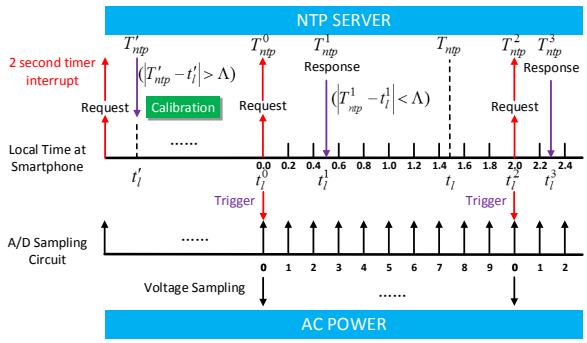

Fig. 4. Timestamps and time synchronization strategy

are received by the smartphone, our application would create a new asynchronous Android task to estimate the operating frequency from these samples.

4) **Graphic interface component.** The curves of frequency and voltage information are visually displayed at the smartphone. The Android library "AChartEngine" is used for such visualization. The graphic interface component is placed in the main thread.

V. NTP-based Time Synchronization

The NTP protocol is widely used in current computing systems, such as the Windows Time Service, with a timing accuracy at the order of 10 ms. Conventional wisdom has adopted NTP for time synchronization in power grid frequency monitoring, but has the monitoring error around 0.2 Hz [15] due to the low timing accuracy of NTP. To prevent such low timing accuracy from affecting the frequency monitoring, we do not directly apply NTP to frequency estimation. Instead, we propose to utilize the NTP timing information to calibrate the local clock drift, and to provide globally synchronized timestamps to the measurement results. The proposed time synchronization strategy is illustrated in Fig. 4.

A. Local Clock Calibration

The local clock of a smartphone will continuously drift due to the dynamic characteristics of the crystal oscillator, as well as various environmental factors such as temperature. As a result, the actual time period for each AC waveform sampling cycle may not be accurately set as expected. For example, a time period set to be 2000ms by the smartphone may be actually 1998ms or 2001ms due to the local clock drift. Such inaccurate sampling frequency will result in the residue problem [16], i.e., the position of the first sample in one sampling cycle is different from that in another cycle, and the residue could be accumulated over time. To address this residue problem, our system starts a new sampling cycle every time when having sent out a NTP request, and hence guarantees the position of the first sample in each sampling cycle are the same in time. Correspondingly, the length of one sampling cycle is set to be 2 seconds, which is as twice as the period of the PPS signal. More frequent NTP requests than once every 4 seconds will be considered as attempting a Denial-of-Service (DoS) attack and hence denied by the NTP server [17]. Therefore, to avoid the failure of NTP queries, the system will alternate the NTP servers to be requested so that one NTP server be requested from the system once in more than 10 seconds.

Each time when the smartphone triggers a sampling cycle, it calibrates its local clock using the received NTP timing information through comparison between the returned NTP timestamp T_{ntp} and the corresponding local time t_l. If $|T_{ntp} - t_l| > \Lambda$ which is the upper bound of NTP timing error, we will calibrate the local timer triggering the sampling cycle, i.e., use a new number rather than 2,000 milliseconds to setup the local timer for triggering the sampling cycles. More specifically, assuming that the local time of the most recent calibration in the past is t'_l and its corresponding NTP time is T'_{ntp}, the new setup time length V' for the local timer (in milliseconds) is defined as follows:

$$V' = \begin{cases} 2000 \cdot (t_l - t'_l)/(T_{ntp} - T'_{ntp}), & \text{if } |T_{ntp} - t_l| > \Lambda \\ V, & \text{Otherwise} \end{cases} \tag{1}$$

where V is the current setup value of the timer.

At the meantime, the local system time is also updated. For example, in Fig. 4, when having received the NTP timing information and found that $|T'_{ntp} - t'_l| > \Lambda$, we change the local time from t'_l to T'_{ntp}.

B. Globally Synchronized Timestamps Calculation

With NTP timing information, we recursively compute the timestamp of the current sampling cycle via proportional estimation from the previous cycle. We assume that the local clock drift within one sampling cycle is negligible. As a result, the timestamp of the first sample in one sampling cycle, which is also the start of the current sampling cycle, as well as the end of the previous sampling cycle, can be estimated from the NTP response and the corresponding local time. For example, in Fig. 4, the NTP time corresponds to t_l^2 can be estimated as:

$$T_{ntp}^2 = T_{ntp}^3 - \frac{t_l^3 - t_l^2}{t_l^3 - t_l^1} \cdot (T_{ntp}^3 - T_{ntp}^2) \tag{2}$$

VI. Performance Evaluation

To evaluate the accuracy and effectiveness of frequency monitoring of our proposed system, we test our system against the traditional FDR device. The system setup is shown in Fig. 5. Both standard power generator and regular AC wall power are used in our experiments.

Fig. 5. Experiment setup

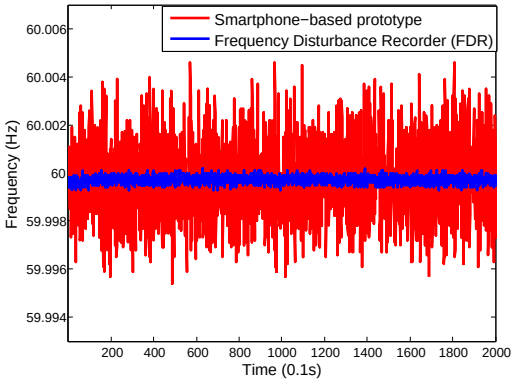

Fig. 6. Results of frequency monitoring over 60Hz function generator

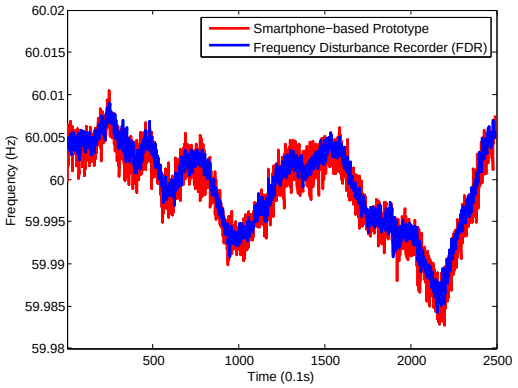

Fig. 7. Results of frequency monitoring over 120V wall power

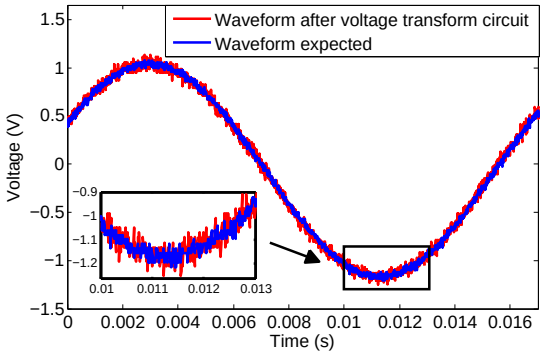

Fig. 8. Waveforms before and after the voltage transform circuit

First, the frequency measurement result over standard 60 Hz power generator is shown in Fig. 6, and the Agilent AC power source 6811B is used to generate 60 Hz, 120V AC power. The standard deviation of the measurement of our system is 1.70 mHz, while that of the FDR device is 0.32 mHz. Second, the frequency measurement results over the 120V AC wall outlet are shown in Fig. 7. We can see our system is able to efficiently capture the trends of frequency deviations over time. Meanwhile, our system produces an 1.7 mHz standard deviation from the FDR measurements being used as the reference.

The application executed on Samsung Nexus S will consume 7% CPU load under idle state, and will run in background when other operations are in progress. The traditional usage of the smartphone, such as voice call, short message will not be interfered by the execution of the application.

Currently, the frequency monitoring accuracy of our system is less than that of FDR due to a couple of reasons. First, the random noise in the power signal was amplified by the voltage transform circuit in our system, and accounted for over 6% of the voltage amplitude. The expected waveform and the waveform after the voltage transform circuit are shown in Fig. 8. Noises are observable especially on the peak of the waveform. This could result in inaccurate measurement of the phase angle, thereby affecting the frequency estimation which is mainly computed from the differentiation of phase angles. Second, timing error exists in the timestamps compared to the real UTC time. That is, the time point of a frequency measurement may not be exactly aligned with its real timestamp. Third, to accommodate the data format of FNET and being able to integrate with NET framework, a curve fitting method is used to estimate the frequency points only at integral 100 millisecond points, such as 06:04:05.2, 06:04:05.3, etc, but may incur additional error due to the limited granularity of curve fitting. Fourth, due to the involvement of both inductive and capacitive components such as transformers and analog filters with different time constants, possible phase lag or advance may be introduced into the frequency monitoring. This may induce a constant time deviance between measurements of our system and the FDR.

VII. Related Work

The power grid frequency and phase angle are generally measured from samples of the voltage waveform. Several algorithms such as zero-crossing techniques, least-square approximation methods [18], Fast Fourier Transform (FFT) [19], Kalman filter methods [20], and phasor-based methods [13], [21], [12] have been proposed for such measurement. To ensure the measurement accuracy, the sampling rate should be in the range of 720-1920 Hz (12-32 data points per cycle), and the accuracy of time synchronization needs to be close to 1 microsecond. Most of current PMUs achieve such timing accuracy by using the GPS system.

A NTP-synchronized Wide Area Frequency Measurement System (WAFMeS) has also been implemented [15]. The architecture of WAFMes consists of three components: Frequency Measurement Devices (FMD), NTP synchronized client side computers and a central server. The functionality of

the FMD is similar to that of the voltage transform circuit in our system, while the client side computers behave as the smartphone in our system. The frequency estimation in WAFMeS is based on zero-crossing detection algorithm. WAFMeS is able to detect the large swing disturbance at the granularity of 0.2 Hz. However, its flexibility and accessibility is restricted, and its accuracy of frequency estimation is too low to be applied to the U.S. power grid with much higher stability and smaller disturbances.

To further increase the timing accuracy without relying on the GPS system, extensive research has been done on harvesting the timing information from the GSM cellular communication system [22]. Since the GSM base stations are strictly synchronized with a single timing source of an absolute accuracy better than 0.05 microseconds [23], GSM signal is able to achieve an equivalent timing accuracy as the GPS signal. Therefore, in the future, we will incorporate the GSM timing signal harvesting module to our prototype, and take advantage of the GSM timing signal as an alternative of GPS signal to achieve more accurate power grid monitoring.

VIII. Conclusion and Future Work

In this paper, we present the design and implementation of our smartphone-based power grid frequency monitoring system. In this system, we proposed to use NTP instead of GPS as the source for time synchronization. The proposed time synchronization approach significantly reduces the system timing error, which is sufficiently low for ensuring precise frequency monitoring on the power grid. Experiments compared with FDR devices show the accuracy and effectiveness of the system on frequency monitoring. The system can be widely deployed as a complementary of the FDRs. The wide-area deployment of power grid monitoring devices will increase the accuracy of abnormal detection and location.

Our future work focuses on further improving our frequency monitoring system, measuring the phase angles of the power grid, and integrating more functionalities of power grid monitoring onto mobile platforms. First, we will improve our frequency monitoring system by fabricating the MCU board and the voltage transform circuit into one PCB board, so that our monitoring system could be integrated into the smartphone charger for better accessibility. We will also improve our design of the voltage transform circuit to efficiently suppress the random noise contained in the power voltage signal. Second, we aim to further improve the accuracy of time synchronization which is necessary for precise monitoring of phase angles and cannot be achieved by NTP. Simply speaking, a 15 milliseconds timing error, which is usually the upper bound of NTP timing error, corresponds to 330 degrees of phase angle error in a 60 Hz system. An alternative high-accuracy timing source is the GSM signal, and we will extract the timing information from the GSM signal in a low-cost yet efficient manner. Third, our system will be further extended to incorporate more functionalities such as power quality measurement that monitors power grid operations in a much wider range of frequency spectrum.

References

[1] J. S. Thorp, C. E. Seyler, and A. G. Phadke, "Electromechanical wave propagation in large electric power systems," *Circuits and Systems I: Fundamental Theory and Applications, IEEE Transactions on*, vol. 45, no. 6, pp. 614–622, 1998.

[2] V. Venkatasubramanian, H. Schattler, and J. Zaborszky, "Fast time-varying phasor analysis in the balanced three-phase large electric power system," *IEEE Transactions on Automatic Control*, vol. 40, no. 11, pp. 1975–1982, 1995.

[3] Y. Zhang, P. Markham, T. Xia, L. Chen, Y. Ye, Z. Wu, Z. Yuan, L. Wang, J. Bank, J. Burgett *et al.*, "Wide-area frequency monitoring network (FNET) architecture and applications," *IEEE Transactions on Smart Grid*, vol. 1, no. 2, pp. 159–167, 2010.

[4] R. M. Gardner and Y. Liu, "FNET: A quickly deployable and economic system to monitor the electric grid," in *IEEE Conference on Technologies for Homeland Security*, 2007, pp. 209–214.

[5] C. W. Gellings, M. Samotyj, and B. Howe, "The future's smart delivery system," *IEEE Power and Energy Magazine*, vol. 2, no. 5, pp. 40–48, 2004.

[6] F. Giraud and Z. M. Salameh, "Steady-state performance of a grid-connected rooftop hybrid wind-photovoltaic power system with battery storage," *IEEE Transactions on Energy Conversion*, vol. 16, no. 1, pp. 1–7, 2001.

[7] A. Armenia and J. H. Chow, "A flexible phasor data concentrator design leveraging existing software technologies," *IEEE Transactions on Smart Grid*, vol. 1, no. 1, pp. 73–81, 2010.

[8] L. Wang, J. Burgett, J. Zuo, C. C. Xu, B. J. Billian, R. W. Conners, and Y. Liu, "Frequency disturbance recorder design and developments," in *Power Engineering Society General Meeting, 2007. IEEE.* IEEE, 2007, pp. 1–7.

[9] C. Xu, "High accuracy real-time gps synchronized frequency measurement device for wide-area power grid monitoring," Ph.D. dissertation, Virginia Tech, 2006.

[10] D. L. Mills, "Internet time synchronization: the network time protocol," *Communications, IEEE Transactions on*, vol. 39, no. 10, pp. 1482–1493, 1991.

[11] L. Wang, J. Fernandez, J. Burgett, R. W. Conners, and Y. Liu, "An evaluation of network time protocol for clock synchronization in wide area measurements," in *Power and Energy Society General Meeting-Conversion and Delivery of Electrical Energy in the 21st Century, 2008 IEEE.* IEEE, 2008, pp. 1–5.

[12] X. Zhang, "High precision dynamic power system frequency estimation algorithm based on phasor approach," Ph.D. dissertation, 2004.

[13] A. G. Phadke, J. S. Thorp, and M. G. Adamiak, "A new measurement technique for tracking voltage phasors, local system frequency, and rate of change of frequency," *IEEE Transactions on Power Apparatus and Systems*, no. 5, pp. 1025–1038, 1983.

[14] MAXIM Integrated (2007), "MAX3421E, usb peripheral/host controller with spi interface," copyright Maxim Integrated Products.

[15] K. A. Salunkhe and A. Kulkarni, "A wide area synchronized frequency measurement system using network time protocol," in *Proceedings of the 16th National Power System Conference*, 2010, pp. 266–271.

[16] J. Zuo, "The frequency monitor network (fnet) design and situation awareness algorithm development," Ph.D. dissertation, Virginia Polytechnic Institute and State University, 2008.

[17] "NIST internet time servers," http://tf.nist.gov/tf-cgi/servers.cgi.

[18] A. A. Girgis and W. L. Peterson, "Adaptive estimation of power system frequency deviation and its rate of change for calculating sudden power system overloads," *IEEE Transactions on Power Delivery*, vol. 5, no. 2, pp. 585–594, 1990.

[19] T. Lobos and J. Rezmer, "Real-time determination of power system frequency," *IEEE Transactions on Instrumentation and Measurement*, vol. 46, no. 4, pp. 877–881, 1997.

[20] P. K. Dash, A. K. Pradhan, and G. Panda, "Frequency estimation of distorted power system signals using extended complex kalman filter," *IEEE Transactions on Power Delivery*, vol. 14, no. 3, pp. 761–766, 1999.

[21] J. Chen, "Accurate frequency estimation with phasor angles," *Master thesis, Virginia Tech*, 1994.

[22] J. K. Brown and D. D. Wentzloff, "A GSM-Based clock-harvesting receiver with -87 dbm sensitivity for sensor network wake-up," *IEEE Journal of Solid-State Circuits*, vol. 48, no. 3, pp. 661–669, 2013.

[23] M. Mouly, M.-B. Pautet, and T. Foreword By-Haug, *The GSM system for mobile communications*. Telecom Publishing, 1992.